

Decay and polarization properties of the top quark

R. H. Dalitz

Department of Theoretical Physics, Oxford University, 1 Keble Road, Oxford OX1 3NP, United Kingdom

Gary R. Goldstein

Department of Physics, Tufts University, Medford, Massachusetts 02155

(Received 1 November 1991)

Polarization and angular distributions in the decay sequence $t \rightarrow bW^+, W^+ \rightarrow l^+\nu_l$ are discussed for the standard model. Top quarks from $e^+e^- \rightarrow t\bar{t}$ are predicted to have large polarization but, even if not, the parity-violating effects in this decay chain are large and will test closely the detailed spin structure of the electroweak interactions involving the top quark. A means of analyzing $t\bar{t}$ decays following $t\bar{t}$ production in hadronic interactions is developed, leading to an illuminating construction. Its application is illustrated by the analysis of the candidate for top-antitop pair creation in $\bar{p}p$ collisions found by the Collider Detector at Fermilab (CDF) at 1.8 TeV center-of-mass energy. If this is really $t\bar{t}$ production, then the top-quark mass would be 125^{+19}_{-11} GeV/ c^2 .

PACS number(s): 14.80.Dg, 13.20.Jf, 13.88.+e

I. INTRODUCTION

The heavy quarks $Q=c, b,$ and t have important individual differences in physics. This is particularly evident in their polarization phenomena. In two earlier papers [1,2], we have discussed the polarization properties of c and b jets, finding that the usual hadronization processes effectively depolarize the heavy quark Q ($=c$ or b) since it always reaches the 0^- state of $(\bar{u}, Q), (\bar{d}, Q),$ or (\bar{s}, Q) before the quark Q decays. For c jets we were able to find a mechanism by which some effects characteristic of Q polarization might show up in (πD) final states with mass $\approx m(D^*),$ but we showed that there were good reasons why even this effect could be only rather small (certainly less than 10^{-3}). For b jets this mechanism was not a real possibility either, the reason being that the γ rays emitted in the dominant B^* decay mode $B^* \rightarrow B\gamma$ are swamped by a general background of γ rays from other sources (especially $\pi^0 \rightarrow \gamma\gamma$ decays) in the same jet. However, for the processes $e^+e^- \rightarrow \bar{c}c \rightarrow \bar{D}^*D^*X,$ a strong polarization correlation was predicted for the \bar{D}^*D^* final states, which should be verifiable when adequate statistics become available. For the processes $e^+e^- \rightarrow \bar{B}B^*X,$ a similar effect was predicted, but the practical difficulties against its observation and measurement appeared quite overwhelming.

The situation is quite different for t and \bar{t} quarks. It is now known empirically [3] that the top quark t is very heavy, more than 89 GeV/ c^2 . Indirect theoretical arguments [4], based on higher-order corrections with the standard model, suggest that its mass may be substantially higher than this lower limit, most likely in the region of 150 ± 30 GeV/ c^2 . In this situation its dominant decay process will be

$$t \rightarrow b + W^+, \tag{1.1}$$

where W denotes the electroweak boson of mass 80.6(4)

GeV/ $c^2,$ through the electroweak interactions, as many authors have noted [5,6]. Since the U_{tb} element of the Kobayashi-Maskawa matrix is essentially unity, certainly to the accuracy needed here, this lifetime can be predicted rather reliably for given mass $m_t,$ and the values obtained are shown in Fig. 1 as a function of $m_t,$ following the calculation of Gilman and Kauffman [7]. These values represent upper limits on the total lifetime $\tau_t,$ since it is not excluded that t may have additional decay

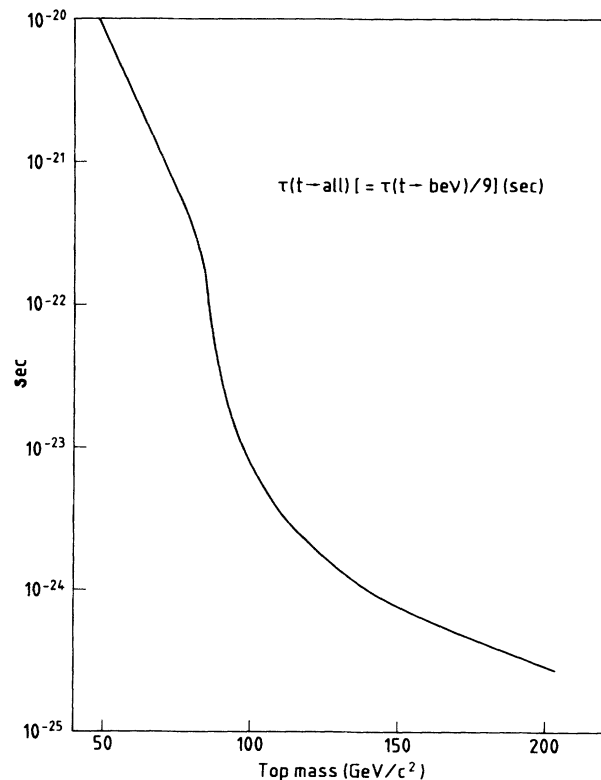


FIG. 1. Total top-quark lifetime as a function of its mass $m_t.$

modes, involving particles not yet detected, a possibility which should not be ruled out of consideration. For $m_t \approx 150 \text{ GeV}/c^2$, the partial lifetime for the mode (1.1) is 7.8×10^{-25} sec, which corresponds to a natural width $\Gamma(t)$ of about 850 MeV.

The rapidity of this decay (1.1) has major consequences for the hadronization of the t quark, as was first noticed by Bigi *et al.* [6]. The magnitude of $\Gamma(t)$ effectively rules out the possibility of a toponium spectroscopy; for toponium, the decay width is $2\Gamma(t)$, thus of order 1700 MeV for $m_t = 150 \text{ GeV}/c^2$, and this is much larger than the energy separation between the $(2S)$ and $(1S)$ ($t\bar{t}$) states. The measurement of $R = (e^+e^- \rightarrow \text{hadrons}) / (e^+e^- \rightarrow \mu^+\mu^-)$ will show, at best, only very broad humps at the lowest (nS) ($t\bar{t}$) states, without detailed structure. There will be no γ rays from transitions between toponium states. For the bare top states (\bar{u}, t), (\bar{d}, t), and (\bar{s}, t), the situation will be similar. Because of the large value of m_t , the energy separation between $T^*(^3S_1)$ and $T(^1S_0)$ states is estimated to be of the order of 5–10 MeV. Top decay in these systems will occur at rates so many orders of magnitude faster than γ -ray transitions between them that the depolarization mechanism effective for c and b systems does not operate for the corresponding t -quark states.

The hadronization processes which gives rise to jet formation when a quark in a hadron is suddenly given a high momentum are also completely modified. In the strong-coupling regime, these processes are well described by the color-flux-tube or color-string model. Following $Q\bar{Q}$ pair creation, Q and \bar{Q} are linked by a string having a constant tension σ , whose empirical magnitude is about 800 MeV/fm, while Q and \bar{Q} separate, with velocity $\beta = [1 - (m_t/E_t)^2]^{1/2}$, E_t being the energy of each in their overall c.m. frame. The t -quark lifetime in this frame is lengthened to $\tau(t)E_t/m_t$, and its mean distance of travel before decay is $c\tau(t)E_t/m_t \approx 0.2(E_t/m_t)$ fm (for a mass of about $150 \text{ GeV}/c^2$, as we show below). In this time the string extends an amount $\approx 2(0.2E_t/m_t)$ fm and therefore receives an energy of $2\sigma(0.2E_t/m_t)$ MeV. This energy is released by breaking the color string, with the creation of a light-quark pair ("quark popping") in the form of a meson, the lightest possibility being the pion, whose mass is $140 \text{ MeV}/c^2$. In the mean the masses relevant are those for π , η , ρ , ω , η' , and, to a lesser extent, for K and K^* , and the meson emitted will have appreciable kinetic energy, so that an energy of ~ 500 MeV per $\bar{q}q$ pair appears to be a reasonable estimate. Experiments possible in this decade are unlikely to have E_t/m_t values exceeding about 1.3. Top-quark decay is so rapid that there can only be about one ($\bar{q}q$) creation event in the time before its decay, and that hadronization is ineffective in these circumstances. This conclusion is comparable with the estimates given by many authors using a wide variety of physical arguments [8].

Such conclusions are favorable for the observation of polarization effects; the complications of hadronization become irrelevant. Whatever momentum and spin information the produced t quark carries will be directly passed on to the decay products. The production and decay of t quarks will provide a probe into the most basic

quark dynamics. With the resulting simplification of top-quark dynamics, it is evident that there are appreciable polarization effects that reflect the basic structure of the standard-model interactions. As we will see below, this applies particularly to the longitudinal and transverse polarization of the top quark predicted to be large in e^+e^- annihilation from the γ - Z^0 interference terms. This polarization will lead to strong lepton asymmetries in the final states.

II. POLARIZED TOP-QUARK DECAY DISTRIBUTIONS

We begin with the electroweak interactions governing the $t \rightarrow bW^+$ and $W^+ \rightarrow l^+\nu_l$ processes. The relevant terms of the interaction Lagrangian have the standard form

$$\bar{b}\gamma_\mu(I - \gamma_5)t W^{\dagger\mu} + \bar{\nu}\gamma_\mu(I - \gamma_5)l W^\mu + \text{H.c.}, \quad (2.1)$$

apart from a numerical factor. The amplitudes $A(\lambda', \Lambda; \lambda)[p, \theta, \phi]$ for a t quark (helicity λ) to transform to a b quark (helicity λ') and a W^+ boson (helicity Λ), obtained by direct calculation from the first term of (2.1), have the following forms, in the top-quark rest frame:

$$A(\mp, 0; \pm) = \frac{\mp p - E_W}{M_W} \sin(\frac{1}{2}\theta) \times \exp(\pm i\frac{1}{2}\phi) [1 \pm p/(E_b + m_b)], \quad (2.2a)$$

$$A(\pm, 0; \pm) = \frac{p \mp E_W}{M_W} \cos(\frac{1}{2}\theta) \times \exp(\pm i\frac{1}{2}\phi) [1 \mp p/(E_b + m_b)], \quad (2.2b)$$

$$A(\pm, \pm 1; \pm) = \sqrt{2} \sin(\frac{1}{2}\theta) \times \exp(\pm i\frac{1}{2}\phi) [1 \mp p/(E_b + m_b)], \quad (2.2c)$$

$$A(\mp, \mp 1; \pm) = \pm\sqrt{2} \cos(\frac{1}{2}\theta) \times \exp(\pm i\frac{1}{2}\phi) [1 \pm p/(E_b + m_b)], \quad (2.2d)$$

the other four amplitudes for $t \rightarrow bW^+$ being identically zero. These expressions hold for decay in the t rest frame; we have denoted the momentum and energy of the b quark by \mathbf{p} and E_b and those for the W meson by $-p$ and E_W (in subsequent discussions, $\mathbf{Q} = -\mathbf{p}$ and $Q_0 = E_W$ will be used for the W three-momentum and energy). Since the t quarks result from $t\bar{t}$ pair creation, in the situations discussed here, it is appropriate to choose the z axis to be along the boost direction from the $t\bar{t}$ center-of-mass frame. The angles (θ, ϕ) specify the direction of the b quark from this decay. Similar expressions hold for the $\bar{t} \rightarrow \bar{b}W^-$ decay amplitudes, the relationship between them being

$$\bar{A}(\lambda_{\bar{b}}, \Lambda; \lambda_{\bar{t}}) = [A(-\lambda_{\bar{b}}, -\Lambda; -\lambda_{\bar{t}})]^*. \quad (2.3)$$

We note that the transitions of W^+ states with helicity $+1$ are substantially suppressed relative to those for W^+ states with helicity $\Lambda=0$ and -1 , for either t helicity. This follows from the parity-violating left-hand couplings in the interaction Lagrangian (2.1); the emitted b quark

has left-handed coupling, and so its helicity is dominantly negative. If $m_b = 0$ held, only the b -quark helicity state ($-\frac{1}{2}$) would enter in the coupling (2.1), and this would limit the helicity of the oppositely directed W^* boson to the values 0 and -1 .

The decay rate for unpolarized t decay to bW^+ is obtained (apart from a constant numerical factor) from the sum

$$\sum_{\Lambda} \sum_{\lambda_b, \lambda_t} |A(\lambda_b, \Lambda; \lambda_t)|^2, \quad (2.4)$$

from which we can pick out the contributions to each final W helicity state Λ . For methodological reasons it is convenient to express these rates in a form valid whether the W boson is on shell or off shell, although the off-shell contributions are negligible when the top mass m_t is more than several W -boson halfwidths ($\Gamma_W \approx 1.25$ GeV) above the bW^+ threshold. They are constructed here by multiplying the relevant (amplitude)² from (2.4) by the bW^+ phase space and expressing the result in integral form, the variable of integration being Q^2 , where Q^2 denotes $(Q_0^2 - Q^2)$ for the W bosons and Q_μ is the energy-momentum four-vector delivered to the W boson in the t rest frame. The resulting forms are

$$\Gamma_{00} = \frac{G_F^2 m_t^5}{24\pi^3} \int_0^{(m_t - m_b)^2} dQ^2 \frac{M_W^4 |Q|}{(Q^2 - M_W^2)^2 + (M_W \Gamma_W)^2} \times [Q^2(1 - Q_0/m_t) + 2Q^2], \quad (2.5a)$$

$$\Gamma_{\pm\pm} = \frac{G_F^2 m_t^5}{24\pi^3} \int_0^{(m_t - m_b)^2} dQ^2 \frac{M_W^4 |Q|}{(Q^2 - M_W^2)^2 + (M_W \Gamma_W)^2} \times [Q^2(1 - Q_0/m_t) \mp Q^2|Q|/m_t], \quad (2.5b)$$

where $\Gamma_{\Lambda\Lambda}$ denotes the transition rate for $t \rightarrow bW_\Lambda^+$, i.e., to a final W^+ -boson state with helicity Λ . We note that the transition rate to helicity $\Lambda = -1$ is different from that to $\Lambda = +1$, anticipated in the remarks just above as a result of parity violation. Numerical values of these partial widths for definite W helicity are given in Fig. 2. For mass m_t near 120 GeV/ c^2 , the $\Lambda = 0$ and -1 rates are comparable in magnitude, but for mass 160 GeV/ c^2 the $\Lambda = 0$ rate is twice that for $\Lambda = -1$. As m_t increases still further, the $\Lambda = 0$ rate becomes increasingly dominant and this parity-violation polarization effect would become increasingly difficult to measure. We note that the $\Lambda = +1$ decay rate is always small compared with the $\Lambda = 0$ and -1 decay rates, the $\Lambda = +1$ decay rate reaching its maximum value only at the threshold for real W production, where the nonzero value of the b -quark mass allows the b quark to be slow and thus to have both helicity states possible. The form (2.5a) has been given by Gilman and Kauffman, but they did not separate the $\Lambda = +1$ and -1 terms, given here in (2.5b); this overlooks this strong polarization effect, which is likely to be important for the physical t mass.

Since the t quark is likely to be produced with strong

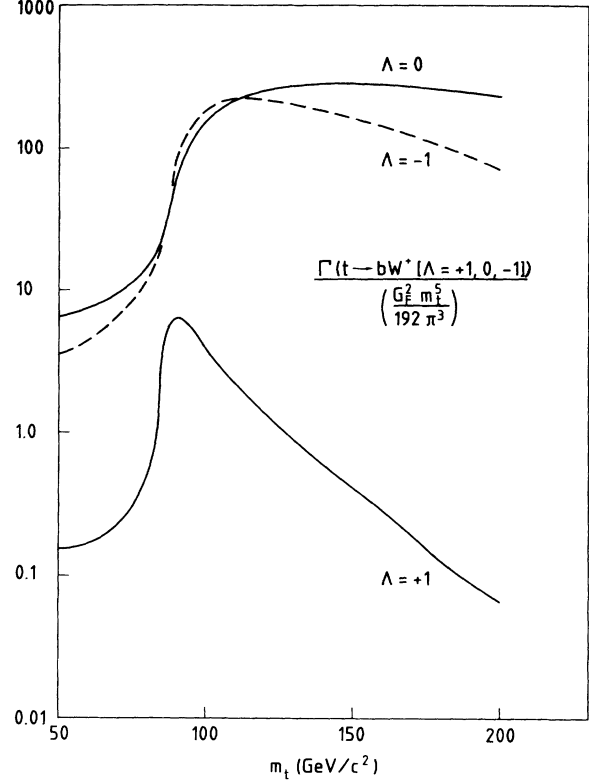


FIG. 2. Partial rates for top-quark decay to bW^+ , for W helicity $\Lambda = +1, 0$, and -1 along its momentum in the top-quark rest frame.

polarization in the $e^+e^- \rightarrow t\bar{t}$ process (see below) and that a strong correlation between polarizations for the t and \bar{t} may be anticipated for a $t\bar{t}$ pair created through hadronic interactions (quark helicity conservation), it is of interest to extend the above results to the case of a polarized t quark. To do this requires the evaluation of the expressions

$$\sum_{\lambda_b, \lambda_t, \lambda'_t} A(\lambda_b, \Lambda; \lambda_t) \rho(\lambda_t, \lambda'_t) A^*(\lambda_b, \Lambda'; \lambda'_t), \quad (2.6)$$

where the density matrix $\rho(\lambda_t, \lambda'_t)$ is for the initial polarized t quark, its values being $(1 \pm \mathbf{P}_t \cdot \boldsymbol{\sigma})_{\lambda_t, \lambda'_t} / 2$, with \mathbf{P}_t pointing along the t polarization in the t -quark rest frame and P_t is the magnitude of that polarization. The expressions (2.5) are modified by an additional polarization term in each square bracket, these becoming as follows:

$$\Gamma_{00}: \dots [Q^2(1 - Q_0/m_t) + 2Q^2 + \mathbf{P}_t \cdot \mathbf{Q}(m_t^2 - m_b^2)/m_t], \quad (2.7a)$$

$$\Gamma_{\pm\pm}: \dots [Q^2(1 - Q_0/m_t) \mp Q^2|Q|/m_t] (1 \pm \mathbf{P}_t \cdot \hat{\mathbf{Q}}), \quad (2.7b)$$

where $\hat{\mathbf{Q}}$ is a unit vector along the W momentum (in the t rest frame). Off-diagonal elements of $\Gamma_{\Lambda'\Lambda}$ are now also required and have the general form (2.5), with square brackets given by

$$\Gamma_{\pm 0} = \Gamma_{0\pm}^* : \cdots [\mathbf{P}_t \cdot (\mp \hat{\boldsymbol{\theta}} - i \hat{\boldsymbol{\phi}}) \mathbf{M}_W \times \{ |\mathbf{Q}| \mp (Q_0 - Q^2/m_t) \} / \sqrt{2}], \quad (2.7c)$$

where $\hat{\boldsymbol{\phi}}$ is a unit vector along $\hat{\mathbf{z}} \times \hat{\mathbf{Q}}$ and $\hat{\boldsymbol{\theta}} = \hat{\boldsymbol{\phi}} \times \hat{\mathbf{Q}}$, with $\hat{\mathbf{z}}$ a unit vector in the direction of the boost required to put the top quark into this rest frame (from the frame in which the t -quark production is naturally specified). The vectors $\hat{\mathbf{z}}$ and $\hat{\mathbf{Q}}$ define a plane in the t rest frame. We see that the component of \mathbf{P}_t along \mathbf{Q} affects the diagonal decay widths [Eqs. (2.7a) and (2.7b)], while the components transverse to \mathbf{Q} produce real or imaginary off-diagonal widths [Eq. (2.7c)] for in or out of the $\hat{\mathbf{z}}\text{-}\hat{\mathbf{Q}}$ plane. The remaining off-diagonal elements $\Gamma_{\pm\mp}$ are identically zero.

To have practical significance, the relative strengths of the contributions from the various W helicity states, which have quite strong dependence on m_t , have to be measured. This can be achieved from observations on the

angular distributions on the lepton from $W^+ \rightarrow \bar{l}^+ \nu_l$ decay, relative to the b -jet axis in the W rest frame. With inclusion of finite-width and off-shell contributions, this angular distribution takes the general form

$$\sum \Gamma_{\Lambda'\Lambda} \Phi_{\Lambda'}^* \Phi_{\Lambda}, \quad (2.8)$$

where the helicity decay amplitudes ϕ_{Λ} are given by

$$\Phi_{\pm 1} = (1 \mp \cos \theta_{\bar{l}bW}) \exp(\pm i \phi_{\bar{l}bW}) / \sqrt{2}, \quad (2.9a)$$

$$\Phi_0 = -\sin \theta_{\bar{l}bW}, \quad (2.9b)$$

the additional suffix W indicating that $\theta_{\bar{l}bW}$ is measured in the W rest frame and the azimuthal angle $\phi_{\bar{l}bW}$ being given relative to the same plane of the t -quark boost and W or b -quark momentum that was defined in the t rest frame via $\hat{\mathbf{z}}$ and $\hat{\mathbf{Q}}$. In terms of the decay-rate matrix $\Gamma_{\Lambda'\Lambda}$ given above, the net angular distribution has the form

$$\begin{aligned} & \Gamma_{00} + \frac{1}{2}(\Gamma_{++} + \Gamma_{--}) - (\Gamma_{++} - \Gamma_{--}) \cos \theta_{\bar{l}bW} + \left[\frac{1}{2}(\Gamma_{++} + \Gamma_{--}) - \Gamma_{00} \right] \cos^2 \theta_{\bar{l}bW} \\ & + \sqrt{2} \sin \theta_{\bar{l}bW} \{ \cos \phi_{\bar{l}bW} \operatorname{Re}[(\Gamma_{+0} - \Gamma_{-0}) \cos \theta_{\bar{l}bW} - (\Gamma_{+0} + \Gamma_{-0})] \\ & - \sin \phi_{\bar{l}bW} \operatorname{Im}[(\Gamma_{+0} + \Gamma_{-0}) \cos \theta_{\bar{l}bW} - (\Gamma_{+0} - \Gamma_{-0})] \}, \quad (2.10) \end{aligned}$$

the last term arising only when the initial t quark has nonzero polarization. The complete angular distribution, for the case of polarization \mathbf{P}_t , is given by the integral (2.5) with square brackets of the following form:

$$\begin{aligned} [\cdots] &= 2 \{ \{ Q^2(1 - Q_0/m_t) + Q^2 + \mathbf{P}_t \cdot \mathbf{Q}(Q_0 - Q^2/m_t) \} \\ & + Q^2 \{ |\mathbf{Q}|/m_t - \mathbf{P}_t \cdot \hat{\mathbf{Q}}(1 - Q_0/m_t) \} \cos \theta_{\bar{l}bW} - (Q^2 + \mathbf{P}_t \cdot \mathbf{Q} Q_0) \cos^2 \theta_{\bar{l}bW} \\ & - M_W \sin \theta_{\bar{l}bW} \{ \cos \phi_{\bar{l}bW} (\mathbf{P}_t \cdot \hat{\boldsymbol{\theta}}) + \sin \phi_{\bar{l}bW} (\mathbf{P}_t \cdot \hat{\boldsymbol{\phi}}) \} \{ |\mathbf{Q}| \cos \theta_{\bar{l}bW} + (Q_0 - Q^2/m_t) \} \}. \quad (2.11) \end{aligned}$$

The vector quantities were defined in the t rest frame, but the overall predicted angular distribution [Eq. (2.11)] is specified in the W rest frame, i.e., the frame in which the lepton and neutrino have zero total three-momentum. Since the neutrino is not detected (and in the full $t\bar{t}$ event there will generally be two hard neutrinos emitted), the W rest frame cannot be specified uniquely, unless the t -quark four-momentum is known. In the $e^+e^- \rightarrow t\bar{t}$ process (see below), the t -quark four-momentum can be deduced when m_t is known, but this is not the case in the hadronic production processes. However, the above angular distributions have no free parameters and can be used in a predictive way for the calculation of distributions to be compared with experimental data.

We now return to the case of the unpolarized t quark. The lepton angular distribution depends both on the mass m_t and on the reference frame in which it is considered, and so, for orientation, we have plotted it in Fig. 3 for mass values m_t from 100 to 180 GeV/ c^2 . In the W rest frame, the lepton distribution is seen to be most forward peaked at lowest m_t and to tend to a symmetric $\sin^2\theta$ distribution as m_t increases and the zero-helicity W boson

begins to predominate. These distributions have also been Lorentz transformed to show their form as seen in the t rest frame; we see that the peak is shifted towards $\theta=90^\circ$. It is instructive to look at the $\cos\theta$ distributions in the t rest frame resulting from the Lorentz transformation of a distribution uniform in the W rest frame, also shown in Fig. 3. Such a uniform distribution could arise from the decay of an unpolarized W (i.e., with $\Gamma_{++} = \Gamma_{--} = \Gamma_{00}$) or from a spin-zero object decaying into a lepton and a neutrino. For a W state with pure helicity $\Lambda=0$, the distribution is precisely a $\sin^2\theta$ distribution, whether viewed in the W or t rest frame; this is the expectation for very massive t quarks.

When these predicted distributions are compared with those for a flat distribution in the W rest frame, we see that the signal in the angular distribution for top decay via the W^+ boson is qualitatively distinguishable, even without knowing the t rest frame precisely. To determine the t mass with precision, a crucial ingredient will be knowledge of the direction of motion of the top quark which is decaying. In the $e^+e^- \rightarrow t\bar{t}$ creation process, the t -quark direction will be roughly indicated as being the

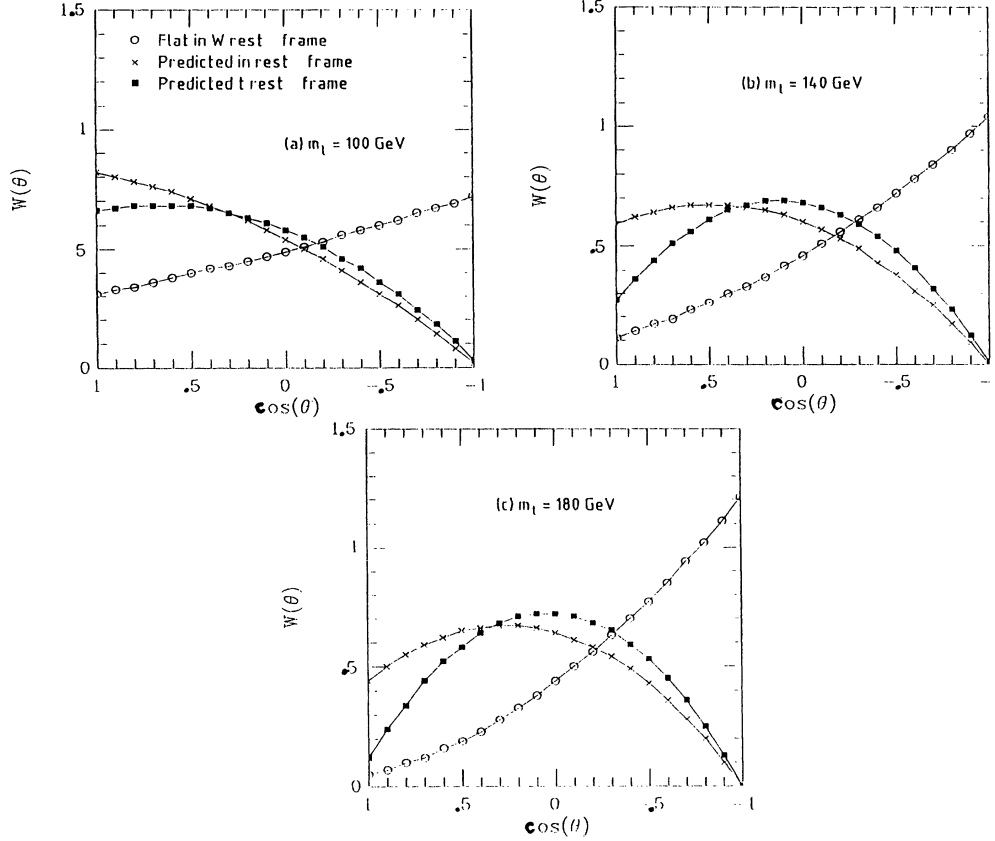


FIG. 3. Angular distribution of the lepton from $W^+ \rightarrow \bar{l}^+ \nu_l$, following $t \rightarrow bW^+$ decay, for three possible values of m_t , where θ is the polar angle relative to the bottom-quark momentum. Crosses, predicted distribution in the W rest frame; squares, predicted distribution shown in the t rest frame; circles, an assumed isotropic distribution in the W rest frame shown in the t rest frame for comparison. All curves are normalized to the same area.

opposite of the \bar{l} decay products when the W^- resulting from the \bar{l} decay decays into a purely hadronic final state. The situation will be more difficult when the top quark is produced hadronically.

III. POLARIZED TOP-QUARK PRODUCTION AND USE [9]

Although we have given some attention to the case of the decay of a polarized top quark in the last section, we return here to discuss the topic in a more general way, along with some production characteristics. We consider the complete two-step process $t \rightarrow bW^+ \rightarrow bl^+\nu_l$, for which the amplitude is

$$[b\bar{\gamma}_\lambda(I-\gamma_5)t] \frac{(g^{\lambda\mu} - Q^\lambda Q^\mu / M_W^2)}{Q^2 - M_W^2 + iM_W\Gamma_W} [\bar{l}\gamma_\mu(I-\gamma_5)\nu], \quad (3.1)$$

where Q_λ denotes the four-vector momentum delivered to the W^+ meson and so to the final $(l^+\nu_l)$ system, so that $Q_\lambda = p_{l\lambda} + p_{\nu\lambda}$. However,

$$Q^\mu [\bar{l}\gamma_\mu(I-\gamma_5)\nu] = (m_\nu + m_l) [\bar{l}(I-\gamma_5)\nu] = 0, \quad (3.2)$$

in the approximation adopted in this paper (i.e., all lepton

masses neglected), and the amplitude (3.1) reduces to the $(V-A)$ four-fermion form

$$[\bar{b}\gamma^\mu(I-\gamma_5)][\bar{l}\gamma_\mu(I-\gamma_5)\nu] / (Q^2 - M_W^2 + iM_W\Gamma_W), \quad (3.3)$$

where we shall drop the last factor, since our attention can be confined to its “on-shell” part, its “off-shell” part being negligible when the top-quark mass exceeds about $100 \text{ GeV}/c^2$. If we now insert Dirac spin functions for t and b states with helicities λ_t and λ_b , respectively, into the first factor of (3.3)—and for the \bar{l}^+ and ν_l spin functions (each with only one helicity state available) into the second factor—we obtain amplitudes $A(\lambda_b, \lambda_t)$ for the complete process $t \rightarrow bl^+\nu_l$. For a partially polarized t particle, described by a density matrix $\rho(\lambda'_t, \lambda_t)$, the rate for the complete process is proportional to

$$\sum_{\{\lambda\}} A(\lambda_b, \lambda'_t) \rho(\lambda'_t, \lambda_t) A(\lambda_b, \lambda_t)^*, \quad (3.4)$$

which may be written

$$\Gamma_t \propto \text{Tr}(U\rho_t), \quad (3.5)$$

where

$$U(\lambda'_t, \lambda_t) = \sum_{\lambda b} A(\lambda_b, \lambda'_t)^* A(\lambda_b, \lambda_t). \quad (3.6)$$

Calculated in the t rest frame, this operator proves to have a remarkably simple form, being proportional to

$$U(\lambda'_t, \lambda_t) \propto (1 + \mathbf{p}_{\bar{l}} \cdot \boldsymbol{\sigma}_t / p_{\bar{l}})_{\lambda'_t, \lambda_t} (p_b \cdot p_\nu). \quad (3.7)$$

It consists of two factors, one which couples the t -quark spin with the lepton momentum vector and the other independent of both the t -quark spin and lepton direction. The importance of this factorization lies in its implication that the angular distribution of the leptons, measured in the t rest frame, allows a direct determination of the t -quark polarization, whatever its direction may be.

This result may be put into a Lorentz-invariant form by making use of the polarization four-vector S for a fermion of mass m , three-momentum \mathbf{p} , and energy E , defined by

$$S = \left[\frac{\mathbf{p} \cdot \mathbf{P}}{m}, \mathbf{P} + \frac{(\mathbf{p} \cdot \mathbf{P})\mathbf{P}}{m(E+m)} \right], \quad (3.8)$$

where $\mathbf{P} = \langle \sigma \rangle$ denotes the polarization vector of the fermion in its rest frame. The covariant form of the first factor of (3.7) is then

$$(p_t - m_t S_t) \cdot p_{\bar{l}}, \quad (3.9)$$

which reduces to $m_t(p_{\bar{l}} - \mathbf{P}_t \cdot \mathbf{p}_{\bar{l}})$ in the limit $\mathbf{p}_t \rightarrow 0$, appropriate to the t rest frame, and $m_t = 0$, as is generally assumed in this paper. The covariant form of (3.7) is therefore found to have the factorized form

$$U = (p_t - m_t S_t) \cdot p_{\bar{l}} (p_b \cdot p_\nu), \quad (3.10)$$

in accord with early work by Kühn [10]. Czarnecki, Jezabek, and Kühn [11] have recently calculated the first-order QCD corrections to U , showing that they do not upset this factorization property substantially.

Using (3.10), the net rate for the two-step transition is

$$\begin{aligned} d\Gamma &= \frac{2G_F^2}{(2\pi)^5 E_t} \frac{d^3 p_b}{E_b} \frac{d^3 p_{\bar{l}}}{E_{\bar{l}}} \frac{d^3 p_\nu}{E_\nu} (p_t - m_t S_t)^\lambda p_{\bar{l}\lambda} \\ &\times \frac{M_W^4}{(Q^2 - M_W^2)^2 + (M_W \Gamma_W)^2} \\ &\times p_b^\mu p_{\nu\mu} \delta^4(p_t - p_b - p_{\bar{l}} - p_\nu), \end{aligned} \quad (3.11)$$

which can be used directly in whichever frame is most convenient.

The processes we are concerned with are two two-body decay processes in succession, for each of which the amplitude is parity violating in a strong and quite definite way. The two successive transition amplitudes are coherent, as far as this is possible when the spin of the b quark is not measured; the electron and neutrino each have only one interacting helicity state, irrespective of

whether or not their spin is measured. The momenta of the product particles in each of the two successive c.m. frames, the t and W rest frames, have definite magnitudes; only the angles are free. In the first process, the angles are θ_{Wt} (angle between \mathbf{p}_W or \mathbf{Q} and the direction of the t boost) and ϕ_{Wt} , the corresponding azimuthal angle, relative to the plane of the t boost and t polarization. The angle ϕ_{Wt} is irrelevant if t is unpolarized or has only longitudinal polarization. In the second process, the angles are $(\theta_{\bar{l}bW}, \phi_{\bar{l}bW})$, the first being the angle between $\mathbf{p}_{\bar{l}}$ in the W rest frame and the momentum \mathbf{p}_b of the outgoing b quark, the second being the azimuthal angle between the plane of $\mathbf{p}_{\bar{l}}$ and \mathbf{p}_b and the plane of the t boost and \mathbf{p}_b . In the W rest frame, $E_{\bar{l}} = E_\nu = M_W/2$; in the t rest frame we have

$$E_W = Q_0 = (m_t^2 + M_W^2 - m_b^2)/2m_t, \quad (3.12a)$$

$$E_b = (m_t^2 - M_W^2 + m_b^2)/2m_t, \quad (3.12b)$$

$$p = |\mathbf{Q}| = \{[m_t^2 - (M_W + m_b)^2] \times [m_t^2 - (M_W - m_b)^2]\}^{1/2}/2m_t. \quad (3.12c)$$

However, as Eq. (3.10) shows, the overall transition rate for the sequence $t \rightarrow bW$, $W \rightarrow \bar{l}\nu$ has a remarkably simple product form. For unpolarized t quarks, the lepton energy spectrum, as measured in the t rest frame, is predicted to have the form

$$\frac{d\Gamma}{dE_{\bar{l}}} = \frac{G_F^2 M_W^3}{2\pi^2 m_t \Gamma_W} \{E_{\bar{l}} [\frac{1}{2}(m_t^2 - m_b^2) - m_t E_{\bar{l}}]\}, \quad (3.13a)$$

for an on-shell W^+ boson. For completeness, we also give the form

$$\begin{aligned} \frac{d\Gamma}{dE_{\bar{l}}} &= \frac{G_F^2 M_W^3}{4\pi^3 m_t} E_{\bar{l}} [\frac{1}{2}(m_t^2 - m_b^2) - m_t E_{\bar{l}}] \\ &\times \int_0^{M_2} dQ^2 \frac{M_W^4}{(Q^2 - M_W^2)^2 + (M_W \Gamma_W)^2}, \end{aligned} \quad (3.13b)$$

which includes the off-shell contributions, the upper limit on the integration being given by

$$M^2 = 2(m_t^2 - m_b^2 - 2m_t E_{\bar{l}})E_{\bar{l}} / (m_t - 2E_{\bar{l}}). \quad (3.13c)$$

This distribution can be Lorentz transformed to other reference frames, of course, but this requires knowledge of the kinematics of the event, as was already discussed above. What is remarkable about (3.13a) is that it depends so simply on the leptonic energy in the t rest frame. Since there is a simple relationship between the antilepton energy $E_{\bar{l}}$ and its angle $\theta_{\bar{l}t}$ in the t rest frame,

$$E_{\bar{l}} = M_W^2 / [2(Q_0 + |\mathbf{Q}| \cos \theta_{\bar{l}t})], \quad (3.14)$$

the distribution (3.13a) can just as well be expressed as an angular distribution

$$\frac{d\Gamma}{d(\cos \theta_{\bar{l}t})} = C \left[m_t^2 - m_b^2 - \frac{m_t M_W^2}{(Q_0 + |\mathbf{Q}| \cos \theta_{\bar{l}t})} \right] / (Q_0 + |\mathbf{Q}| \cos \theta_{\bar{l}t})^3, \quad (3.15)$$

where C is a normalization constant, although its form is not quite so simple. In the W rest frame, the lepton spectrum is the line $E_{\bar{l}W} = M_W/2$, smeared by the finite width Γ_W of the W boson. The form (3.10) implies that the lepton angular distribution in the W rest frame, given in Eq. (2.11), can be written in a factorized form, at least when the distribution is averaged over the azimuth angle $\phi_{\bar{l}b}$ (which is the same as $\phi_{\bar{l}W}$). It may readily be checked that (2.11) then has the equivalent form

$$2(Q_0 - Q^2/m_t + |Q| \cos\theta_{\bar{l}bW})[Q_0 - |Q| \cos\theta_{\bar{l}bW} + \mathbf{P}_t \cdot \hat{\mathbf{Q}}(|Q| - Q_0 \cos\theta_{\bar{l}bW})]. \quad (3.16)$$

In the top-quark rest frame, the simplicity persists when the t quark is polarized. As remarked just above, there is a very direct connection between the lepton energy and its direction $\theta_{\bar{l}b}$, in this frame, given by Eq. (3.14). For polarized top quarks, U still factors, giving the following expression in place of the curly brackets of (3.13a):

$$\{[1 - P_t \cos(\theta_{\bar{l}Pt})](E_{\bar{l}t} \{ \frac{1}{2}(m_t^2 - m_b^2) - m_t E_{\bar{l}t} \})\}, \quad (3.17)$$

where $\theta_{\bar{l}Pt}$ is the angle between \bar{l} and the t polarization, seen in the t rest frame. It may appear that this factorization implies that the t polarization can be deduced from $t \rightarrow W \rightarrow \bar{l}$ angular data, independent of complete observation of the \bar{l} energy spectrum in this frame, but in fact the $\theta_{\bar{l}Pt}$ and $E_{\bar{l}t}$ distributions are linked indirectly. This is illustrated most readily for longitudinal polarization, as we now consider. With a definite value for $E_{\bar{l}t}$ in the t rest frame, the value of $\theta_{\bar{l}b}$ in this frame is fixed according to (3.14), so that the possible values for $\mathbf{p}_{\bar{l}}$ in the t rest frame are limited to a cone about the b - W axis. The angle $\theta_{\bar{l}Pt}$ is therefore limited to lie within the range $[\pm\theta_{Wt} + (\pi - \theta_{\bar{l}b})]$, which is determined by this value of $E_{\bar{l}t}$. In spite of such complications, it remains true that observation of the lepton angular and energy distributions can lead to a determination of the t -quark polarization, as well as provide a check on the detailed form of the transition amplitudes from the standard ($V-A$) model.

The standard model does predict quite strong polarization in the production plane for the top quark produced in the annihilation interactions of unpolarized e^+ and e^- beams, in consequence of the parity-violating element of the Z^0 coupling with $\bar{q}q$ quark pairs. As illustrated in Fig. 4(a), the longitudinal polarization is a strongly varying function of the c.m. angle θ of the top-quark production, being less than -30% in the forward direction and greater than $+60\%$ in the backward direction. There is also a sizable positive transverse polarization in the production plane as shown in Fig. 4(b), reaching over 40% near 90° production angle. It is noted that the polarization predicted has only a weak dependence on the top-quark mass m_t over the range 90 – 180 GeV/c^2 shown in Fig. 4, at least for e^+e^- energies more than several GeV above the production threshold. This has the consequence that a rough separation between forward and backward events will provide t -quark decay events with a definite sign (in the mean) for their longitudinal polarization. The transverse polarization normal to the production plane calculated for the top quark in $e^+e^- \rightarrow t\bar{t}$ production [9] is quite negligible (of order 10^{-4}).

The above remarks hold also for the top antiquark \bar{t} , with the obvious changes appropriate for the transitions $\bar{t} \rightarrow \bar{b}W^-$ and $W^- \rightarrow l^- \bar{\nu}_l$. The relationship is simple in the approximation that the quark momenta are large compared with their masses. Chirality and helicity then nearly coincide and the (V, A) couplings produce pairs with opposite helicity for t and \bar{t} . If the top quark has longitudinal polarization P_t , the accompanying top antiquark will have longitudinal polarization $-P_t$. For $e^+e^- \rightarrow t\bar{t}$, the \bar{t} longitudinal polarization may be read from Fig. 4(a) by rotating it by 180° about the point

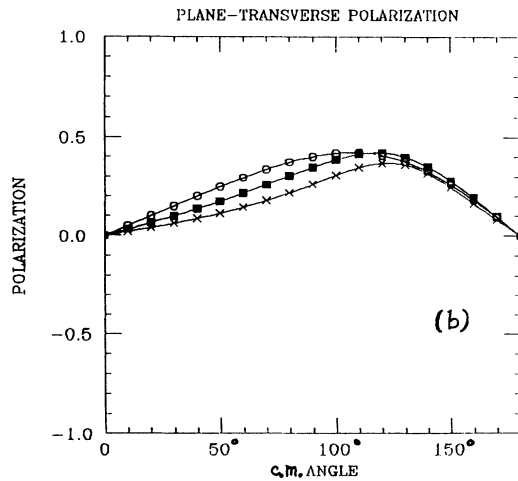
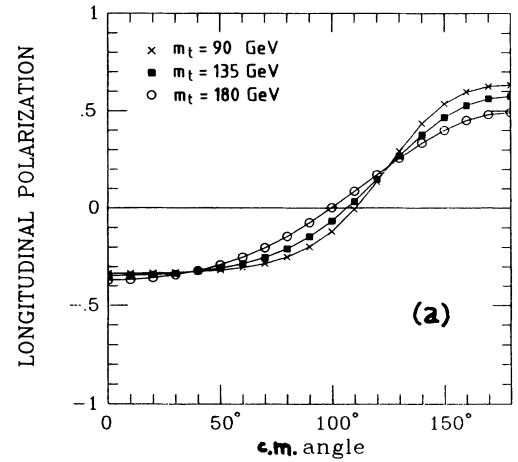


FIG. 4. Top-quark (a) longitudinal polarization and (b) transverse (in the production plane) polarization for the $e^+e^- \rightarrow t\bar{t}$ reaction is given as function of its polar angle relative to e^- , in the e^+e^- rest frame with $E_e = 200$ GeV and for $m_t = 90$ GeV/c^2 (crosses), 135 GeV/c^2 (circles), and 180 GeV/c^2 (squares).

($\theta=90^\circ$, $P_t=0$). This property holds in consequence of CP invariance of the electroweak interactions.

IV. KINEMATIC ANALYSIS OF TOP-QUARK DECAY EVENTS

The events physics will provide us with in the near future will be $t\bar{t}$ pair-creation events. Both particles will rapidly decay, giving $t \rightarrow bW^+$ and $\bar{t} \rightarrow \bar{b}W^-$. The events will be most readily identified if each W boson undergoes leptonic decay, which involves the emission of two rather energetic neutrinos in the event. How can we then hope to analyze these events, in order to determine the top-quark mass and elucidate its production and decay processes? Initially, our remarks will be made with the case of $t\bar{t}$ creation by an electron-positron collider in mind, but we shall discuss the case of proton-antiproton colliders at the end of this section, with a rough analysis of the one candidate event available today.

We consider e^+e^- annihilation for beam energies E . If the t -quark mass m_t were known, the magnitude of the t -quark momentum would be known, although not its direction. If the accompanying \bar{t} decay were entirely hadronic, with $W \rightarrow \bar{q}q'$ giving two jets, the net momentum of its charged products could give a rough estimate of the \bar{t} direction and, therefore, by reversal, that of the t quark, irrespective of whether or not m_t were known. Indeed, if m_t were not known, this estimate of the t direction could provide vital information, leading to a determination of m_t . We return to this point below.

For the present, consider the most favorable case, of a t quark with some energy E , whose decay is $t \rightarrow bW^+$ followed by $W^+ \rightarrow \bar{l}^+ \nu_l$, where the b jet is well defined in energy and direction and the lepton likewise. We denote the four-momenta (three-momenta) of these particles by t (\mathbf{t}), b (\mathbf{b}), and \bar{l} ($\bar{\mathbf{l}}$), with an assumed value for m_t . There are two constraints on these vectors.

(i) The lepton and neutrino result from W decay. Their net four-momentum is necessarily $(t - b)$, so that

$$(\mathbf{t} - \mathbf{b})^2 = (E - E_b)^2 - M_W^2 = R_W^2. \quad (4.1)$$

(ii) The neutrino is massless. Its four-momentum is necessarily $(t - b - \bar{l})$, so that

$$(\mathbf{t} - \mathbf{b} - \bar{\mathbf{l}})^2 = (E - E_b - E_{\bar{l}})^2 = R_\nu^2. \quad (4.2)$$

These equations lead to the construction shown in Fig. 5, based on an origin P . The desired vector \mathbf{t} (denoted by \mathbf{PX}) lies on two spheres, one of radius R_W , centered on B (such that $\mathbf{PB} = \mathbf{b}$), and the other of radius R_ν , centered on L (such that $\mathbf{PL} = \mathbf{b} + \bar{\mathbf{l}}$). If the two spheres do not intersect, then there is no solution; the event cannot fit the decay sequence proposed for it. This requirement will generally provide an absolute lower limit E_0 on the energy E for which this (b jet, \bar{l}^+) event can be interpreted as being due to t -quark decay, whatever m_t may be.

When the spheres intersect, as they do in Fig. 5, any acceptable vector \mathbf{t} must lie on their circle of intersection, which lies on a plane perpendicular to the vector $\bar{\mathbf{l}}$, since we have, from (4.1) and (4.2),

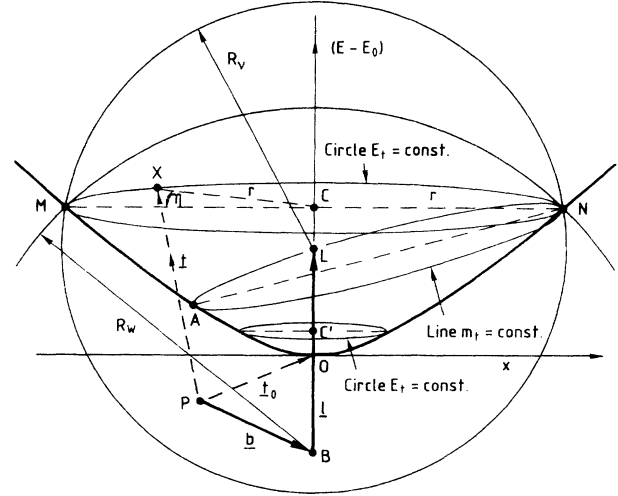


FIG. 5. Momentum vectors \mathbf{b} and $\bar{\mathbf{l}}$ observed in the laboratory frame for bottom quark and lepton, and the construction for locating all top-quark momenta \mathbf{t} such that these three vectors can correspond to the decay sequence $t \rightarrow bW^+$, $W^+ \rightarrow \bar{l}^+ \nu_l$ for a given top-quark mass m_t .

$$\mathbf{t} \cdot \hat{\mathbf{l}} = E - (E_b - \hat{\mathbf{l}} \cdot \mathbf{b}) - M_W^2 / 2E_{\bar{l}}, \quad (4.3)$$

neglecting m_l^2 , where $\hat{\mathbf{l}}$ denotes a unit vector along $\bar{\mathbf{l}}$. As E increases, this plane moves upward along the axis BL (which represents the vector $\bar{\mathbf{l}}$). The radius r of this circle of intersection is obtained from the equation

$$(R_W^2 - r^2)^{1/2} \pm (R_\nu^2 - r^2)^{1/2} = \pm l, \quad (4.4)$$

where l symbolizes the magnitude of $\bar{\mathbf{l}}$ (or $E_{\bar{l}}$). The signs appropriate here depend on the values of \mathbf{b} and $\bar{\mathbf{l}}$; for the case depicted in Fig. 6, the sign on the left-hand side of (4.4) is $(-)$, whereas the sign on the right-hand side is $(+)$. However, in all cases, the magnitude of r is given by

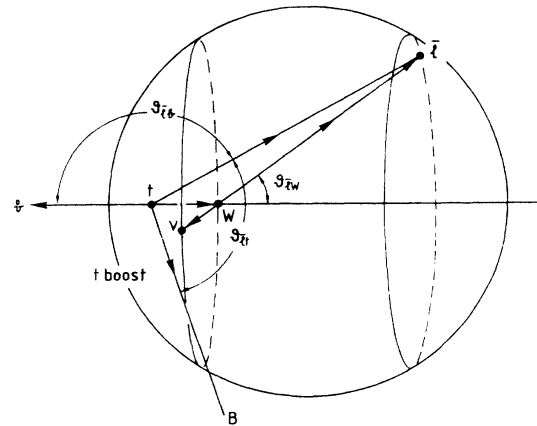


FIG. 6. Lepton momentum l in the W rest frame (angle θ_{lW} with the line tW) and in the top-quark rest frame (angle θ_{lb} with the line lb). $\theta_{\bar{l}}$ is the angle between $\bar{\mathbf{l}}$ and the top-quark boost direction, in the top-quark rest frame, and $\phi_{\bar{l}}$ (not shown in the figure) is the azimuthal angle between the planes $\bar{\mathbf{l}}tW$ and BtW .

$$r^2 = (M_W^2/l)(E - E_0), \quad (4.5)$$

where the constant E_0 is given by

$$E_0 = E_b + E_\tau + M_W^2/4E_\tau, \quad (4.6)$$

irrespective of which (\pm) signs occur. We note that the circle of intersection shrinks to a point when E falls to E_0 , so that E_0 is the lowest energy for which any top quark fit to these b -jet and lepton momenta is possible. As E increases above E_0 , the circles form the surfaces of a paraboloid, as Eq. (4.5) indicates. [If lepton masses are retained, this surface is an ellipsoid, but with a major axis (l/m_l) times its minor axis.]

For the circle MXN , centered at C , and for energy E , the vector PX is the top-quark momentum \mathbf{t} corresponding to the point X . Clearly, PX varies in magnitude as X moves around the circle. Hence the mass $m_t = (E^2 - PX^2)^{1/2}$ varies around the circle. The full paraboloid H gives an infinity of sets (E, \mathbf{t}, m_t) , which can fit the empirical (b jet, \bar{l}) event. It is of interest to determine all of the points for which m_t has a prescribed value. The surface of the paraboloid H may be parametrized by

$$\mathbf{t} = \mathbf{t}_0 + (E - E_0)\hat{l} + x\mathbf{i} + y\mathbf{j}, \quad (4.7a)$$

where \mathbf{t}_0 is the top-quark momentum for the limiting energy E_0 , given by

$$\mathbf{t}_0 = \mathbf{b} + (1 - M_W^2/4E_\tau^2)\bar{l}, \quad (4.7b)$$

and $(x, y) = (r \cos \eta, r \sin \eta)$, the phase angle η being defined in Fig. 5. Note that MCN lies in the plane PBL containing the vectors \mathbf{b} and \bar{l} and that the unit vector \mathbf{i} is defined to lie along CM , \mathbf{j} being perpendicular to this plane. Then

$$m_t^2 = E^2 - \mathbf{t}^2 = (E - E_0)(2E_0 - M_W^2/E_\tau - 2\mathbf{t}_0 \cdot \hat{l}) + 2x\mathbf{i} \cdot \mathbf{t}_0 + m_0^2, \quad (4.8a)$$

where

$$m_0^2 = m_b^2 + M_W^2 + 2b \cdot l(1 - M_W^2/4E_\tau^2) + M_W^2 E_b / E_\tau. \quad (4.8b)$$

The points P for a definite m_t therefore lie on a plane section of the paraboloid H . The perpendicular to this plane lies parallel to the plane of \mathbf{b} and \bar{l} , its normal making an angle θ with the vector \bar{l} , where

$$\tan \theta = -\mathbf{b} \cdot \mathbf{i} / (E_b - \mathbf{b} \cdot \hat{l}). \quad (4.9)$$

The plane section obtained is necessarily an ellipse. We note there is only a single infinity of solutions for a definite mass m_t and that the t -quark energy E can then lie only between two limits $E_{\min} < E < E_{\max}$, corresponding to the highest and lowest points of this plane section. These two extreme points lie on the vertical plane of symmetry MON , the plane of \mathbf{b} and \bar{l} .

The construction shown in Fig. 5 may be used in a number of ways.

(a) *Electron-positron colliders.* In this case the energy

E is set by the mode of operation of the machine. The $\bar{t}\bar{t}$ threshold at $2m_t$ could conceivably be signaled by a sudden rise in the ratio $R = (\text{hadrons})/(\mu^+\mu^-)$ as E increases through $2m_t$, but this is unlikely to be the case. The cross section for $(t + \bar{t})$ unbound states will be small near threshold and the onset of $\bar{t}\bar{t}$ pairs difficult to detect, as a function of energy. We recall that the toponium states below this threshold will be very broad, each overlapping its neighbors. It may be possible to see the $(\bar{t}\bar{t})$ $1S$ state as a broad rise and fall of R , but its full width may be comparable with the separation between it and the $2S$ level. The higher (nS) levels will merge into a continuous spectrum, perhaps with some degree of modulation. [Already in the case of bottomonium, it has not been possible to locate precisely the $\bar{b}b$ threshold solely from measurements of R . It has only been possible to bracket this threshold by noting that $\Upsilon(4S)$ is a broad level (width about 24 MeV), whereas $\Upsilon(3S)$ is a narrow level (width about 24 keV), but this line of argument will not be available for the bound $\bar{t}\bar{t}$ states, in view of the large number of (nS) states predicted and the great breadths predicted for them.]

(i) As just remarked above, the knowledge of E and of the (b jet, l^+) momenta allows an infinity of values for m_t , between two extreme limits (corresponding to the points M and N in Fig. 5, where x takes the values $+r$ and $-r$, respectively). One further datum is needed. This might be provided from a rough indication of the direction of \mathbf{t} , the t -quark three-momentum, as the opposite of $\bar{\mathbf{t}}$, the three-momentum of the other member of the (\bar{t}, t) pair, if the \bar{t} decay involves no neutrino emission, but gives rise to three hadronic jets (a \bar{b} jet and two jets from $W^- \rightarrow \bar{c}b$ decay). The summed momenta of all the charged particles resulting from this sequence of jets can provide an estimate of the \bar{t} direction adequate enough for this purpose. A line drawn from P in Fig. 5, parallel to $-\bar{\mathbf{t}}$, may (within the empirical uncertainties) intersect the ring MXN , providing for a possible \mathbf{t} fit, determining thereby the value of m_t . If this line (or a cylinder, rather, when empirical uncertainties on the \bar{t} decay are included) does not intersect the ring (torus, when the experimental uncertainties on the t decay are included), the conclusion must be that the event is not an example of $\bar{t}\bar{t}$ creation.

(ii) If the $\bar{t} \rightarrow \bar{b}W^-$ decay is followed by $W^- \rightarrow l^-\bar{\nu}_l$, then we must carry out the above construction also for the \bar{t} decay. The \bar{t} decay event must correspond to a point on the ring for center \bar{C} on paraboloid \bar{H} , just as the t decay event corresponds to a point on the ring for center C on paraboloid H , both rings being constructed for the same energy E . The two paraboloids H and \bar{H} are necessarily different in form since they are based on different b and l^+ momentum values, but the two vectors \mathbf{OP} and $\bar{\mathbf{OP}}$ must sum to zero. If the origin O is placed on O and all momenta involved in the figure constructed on \bar{O} are reversed, the resulting momenta and points being denoted by a prime, then the rings C and \bar{C}' must intersect and the point of intersection should give the same mass value for each ring. In practice, the rings will be tori and there will be a volume of intersection (possibly two separate volumes, if C and \bar{C}' happen to intersect twice, though this is highly unlikely since the two rings C

and \bar{C}' will not lie on the same plane), resulting from the uncertainties in the experimental measurements. If the intersection were found to correspond to differing values for m_t and \bar{m}_t , or if the rings C and \bar{C}' turned out not to intersect, the conclusion would have to be that the e^+e^- annihilation event under study was not of the type $(t+\bar{t})$.

(b) *Proton-antiproton collider.* The situation here is more complicated, because the $\bar{t}t$ rest frame is not known. There are more parameters needed to fit the net $(t+\bar{t})$ event, and the conclusion reached can only be assessed in terms of likelihood. The construction of Fig. 5 can be used for the analysis of the $(b \text{ jet}, \bar{t}^+)$ and $(\bar{b} \text{ jet}, l^-)$ configurations resulting from the t and \bar{t} decays separately, as discussed for the case of $e^+e^- \rightarrow \bar{t}t$ above. For each system there will be many fits, each fit being characterized by two parameters, (E, η) for a t quark and $(\bar{E}, \bar{\eta})$ for a \bar{t} quark. E (\bar{E}) gives the energy of the quark (antiquark) in the laboratory frame and therefore the ring MXN ($M\bar{X}N$) in Fig. 5 on which the corresponding point X (\bar{X}) is located; η ($\bar{\eta}$) gives the angle MCX , as shown in Fig. 5, thus locating the point X (\bar{X}) uniquely. For each fit (E, η) or $(\bar{E}, \bar{\eta})$, the momentum of the quark or antiquark is definite, so that each fit requires a definite mass value m_t or \bar{m}_t .

We shall discuss the procedure to be followed, by using the physical parameters reported [12] for the one candidate $(t+\bar{t})$ production event found by the Collider Detector at Fermilab (CDF) group, given in Table I.

(i) As remarked above, it is always possible to give a definite lower limit on m_t . For the $(b \text{ jet}, \bar{t}^+)$ system, Eq. (A3) and inequality (A8) lead to the result

$$\bar{l} \cdot b = 2685, \quad (4.10a)$$

leading to $m_t \geq 109.2 \text{ GeV}/c^2$. For the $(\bar{b} \text{ jet}, l^-)$ system, the corresponding inequality happens to be a little stronger, the result being

$$l \cdot \bar{b} = 2770, \quad (4.10b)$$

leading to $m_{\bar{t}} \geq 110.0 \text{ GeV}/c^2$.

(ii) A single configuration $(b \text{ jet}, \bar{t}^+)$ can be fitted for arbitrarily large m_t , but the appropriate value for E is then correspondingly large. The configuration of the decay sequence, in the top-quark rest frame, has to be correspondingly special, such as to give these low values for p_b and $p_{\bar{t}}$ and, therefore, less and less reasonable.

(iii) Now we combine the fits for $(b \text{ jet}, \bar{t}^+)$ with those

for $(\bar{b} \text{ jet}, l^-)$ by requiring (a) that the two fits give the same mass, and (b) that the net transverse momentum for the two fits is not unreasonably large, namely,

$$|(\mathbf{p}_t)_{\text{trans}} + (\mathbf{p}_{\bar{t}})_{\text{trans}}| \leq p, \quad (4.11)$$

where we have chosen the limit $p = 0.1m_t$. Abe *et al.* [13] have discussed the generation of transverse momentum for partons and jets by gluon emission from the initial interacting partons, finding a distribution function roughly Gaussian with mean transverse moment of 14%–21% of the outgoing-jet transverse energy. This scales up the result of about 5 GeV/ c at the energy of the CERN collider [14].

For an assumed top-quark mass m_t ($\pm 0.5 \text{ GeV}/c^2$), we have laid out a four-dimensional grid, for E and \bar{E} in steps of 1.0 and 2.0 GeV, respectively, and for η and $\bar{\eta}$ in steps of 5° . We tested every point on the grid, requiring the computer to register those points for which condition (4.11) was satisfied with $p = 0.1m_t$. The acceptable points in the grid clustered in groups, some with particularly low values for p_{trans} . Typical parameter sets, with the lowest values for p_{trans} , have been collected together in Table II, for a series of top-quark mass values. Most of these groups belong to an evolving cluster, varying continuously as m_t increases. The energies E and \bar{E} required increase as m_t increases. Although each configuration $(b \text{ jet}, \bar{t}^+)$ and $(\bar{b} \text{ jet}, l^-)$ can be fitted for arbitrarily large m_t and \bar{m}_t , so that the requirement that $m_t = \bar{m}_t$ can always be met, the quantities which are not input, such as E , \bar{E} , and $(p_t)_{\text{trans}}$, become unreasonably large, requiring rather precise values selected to fit the small input quantities; for example, the condition (4.11) then becomes difficult to meet.

Next, we consider the longitudinal momenta deduced for t and \bar{t} in these pairwise fits. Assuming the fundamental creation process

$$\text{parton} + \text{antiparton} \rightarrow t + \bar{t}, \quad (4.12)$$

we can deduce uniquely x and \bar{x} for the initial parton and antiparton, and the values obtained are also entered in Table II. We note that the values x and \bar{x} are not small. With the Tevatron energy of 1.8 TeV and if this one event we are discussing is really due to $\bar{t}t$ production and decay, it is apparent that this event is most probably generated by the valence quarks q_v of the proton interacting with the valence antiquarks \bar{q}_v of the antiproton. Since a

TABLE I. Measurements by CDF of their “ $t\bar{t}$ candidate” event [12], specified in the laboratory frame, and the proposed identifications (id.) for the leptons and jets observed. E_{trans} denotes “transverse energy,” while η and ϕ denote the pseudorapidity and azimuthal angle in each case.

	p_x (GeV/ c)	p_y (GeV/ c)	p_z (GeV/ c)	E (GeV)	E_{trans} (GeV)	η	ϕ (rad)	id.
e^+	-21.18	23.61	-28.56	42.68	31.72	-0.81	2.30	t
$b \text{ jet}$	18.71	-6.27	25.25	33.26	19.73	1.07	5.96	t
μ^-	-0.62	-43.69	-38.64	58.33	42.54	-0.80	4.70	\bar{t}
μ^+	-1.03	7.94	-28.74	29.83	7.58	-1.96	1.70	$\bar{b} < \bar{t}$
jet	0.74	8.86	-70.12	70.73	8.89	-2.76	1.49	$\bar{b} < \bar{t}$

TABLE II. Shows representative sets of parameters $E(\bar{E})$ (GeV) for t and \bar{t} , $p_T(\bar{t})$ (GeV/ c) the transverse momentum for the (\bar{t}) pair in GeV/ c , and the angle $\eta(\bar{\eta})$ defined as in Fig. 6. $F(x)$ is the parton structure function of the proton; $F(\bar{x})$ is the same evaluated for \bar{x} . $P(\bar{l})$ ($P(l)$) represents the probability for lepton momentum \bar{l} (l) in the W decay following t (\bar{t}) decay, as given in Eq. (2.12a).

m_t	E	η^0	x	\bar{E}	$\bar{\eta}^0$	\bar{x}	$p_T(\bar{t})$	$P(\bar{l})$ [$P(\bar{l})$]	$F(x)$ [$F(\bar{x})$]
112	122.5	220	0.10	320	180	0.39	0.32	0.008	5.26
115	130	225	0.11	350	175	0.42	4.23	0.030	3.78
120	130	280	0.11	230	150	0.29	1.27	0.073	9.90
120	130	215	0.12	390	175	0.47	1.12	0.073	2.28
125	142.5	270	0.125	250	140	0.31	1.50	0.113	7.47
125	142.5	90	0.081	250	220	0.35	2.28	0.113	8.52
132	170	140	0.10	430	200	0.56	1.95	0.155	1.19
132	172.5	210	0.14	465	170	0.57	4.14	0.155	0.75
140	192.5	150	0.12	500	195	0.65	1.46	0.183	0.36
140	195	195	0.15	520	175	0.65	2.87	0.183	0.28
150	222.5	190	0.16	580	175	0.73	0.17	0.200	0.09
170	245	80	0.10	220	300	0.41	2.20	0.186	4.27
200	335	85	0.13	255	330	0.52	3.13	0.142	1.23

typical valence quark carries about $\frac{1}{3}$ of the proton energy, i.e., about 300 GeV, the creation of a $\bar{t}t$ pair with total rest energy of substantially more than 220 GeV/ c^2 (say, 2×150 GeV/ c^2) accounts for a relatively large part of the energy available in the initial \bar{q}_v - q_v system. In Table II we see that the smallest (x, \bar{x}) values required to fit the event, assuming it to be $\bar{t}t$ production and decay, are $\approx(0.08, 0.3)$. These values imply that the sea-quark interactions and the gluon-gluon interactions can make rather little contribution to the rate of $\bar{t}t$ pair creation at 1.8 TeV. As the assumed top-quark mass is increased, the values required for x and \bar{x} to fit this observed configuration of decays soon become greater than can be provided by the proton and antiproton, respectively; in short, the parton-antiparton energies available in these proton-antiproton collisions are no longer sufficient to fit these data, if it is assumed that this one special event is due to top-antitop production. From this argument alone, we can conclude that the top-quark mass is most unlikely to be greater than 200 GeV/ c^2 .

To draw a more positive conclusion, we have made a rough estimate of the relative likelihood of producing a $\bar{t}t$ pair with the observed configuration, for an assumed value for m_t . We will then make use of Bayes's theorem to deduce the relative probability for the top-quark mass to be m_t , given the $(b\bar{l}, \bar{b}l)$ event observed. We include the following factors:

(a) The probabilities $P(E_{\bar{t}}, m_t)$ and $P(\bar{E}_{\bar{t}}, \bar{m}_t)$ of obtaining the (uncorrelated) $E_{\bar{t}}$ and $\bar{E}_{\bar{t}}$ energy values, in the t and \bar{t} rest frames, respectively, deduced for each acceptable fit, using the theoretical expression (3.13).

(b) The values of the structure functions, $F(x)$ for the proton and $F(\bar{x})$ for the antiproton, for the values of x and \bar{x} for each acceptable fit. The structure function is that of Duke and Owens [15] (set 2) for $(u+d)$, with $Q^2 = m_t^2$. The likelihood function is calculated as

$$L(m_t) = \left[\sum_i F(x_i) F(\bar{x}_i) P(E_{\bar{t}}, m_t) (E_{\bar{t}}, m_t) \right] / N(m_t), \quad (4.13)$$

where the sum is taken over all matched pairs (t, \bar{t}) defined by the parameters (E, η) and $(\bar{E}, \bar{\eta})$, respectively, having masses m_t and $m_{\bar{t}}$ equal within ± 0.5 GeV, but restricted to those pairs having $p_{\text{trans}} < 0.1 m_t$. The denominator denotes the total number of matched pairs found, without restriction on their overall p_{trans} . On this simple-minded basis, we obtain an estimate for $L(m_t)$ for this one event, based on 1000–2000 matched pairs for each m_t ($m_t = 112$ – 132 GeV/ c^2 in steps of 1 GeV/ c^2 and 134 – 150 GeV/ c^2 in steps of 2 GeV/ c^2). Even with these large numbers of matched pairs, there are still considerable statistical fluctuations in the calculated $L(m_t)$, which requires some smoothing, our final evaluation of $L(m_t)$ being shown here in Fig. 7. Using Bayes's theorem, our conclusion is that the top-quark mass is about 125 GeV/ c^2 , with limits 115–144 GeV/ c^2 at the level of one standard deviation.

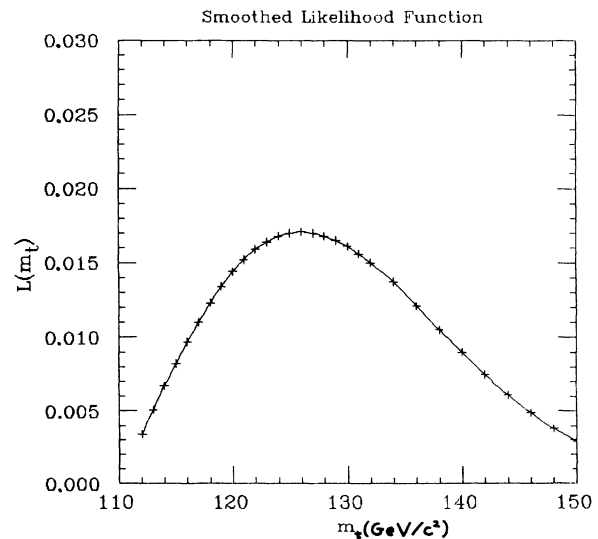


FIG. 7. Estimate of the Bayesian probability for top-quark mass m_t on the basis of a fit to the single CDF candidate event, as discussed in the text.

V. CONCLUSION

As a result of the rapid decay, $t \rightarrow bW$ through the electroweak interaction, predicted for the top quark by the standard model, its polarization is little affected by the hadronization. This decay reflects the structure of this ($\bar{b}t$) interaction, and it gives rise to a strongly polarized W boson, whose polarization can be determined from observations on its $W \rightarrow l\nu$ decay mode. Studies of these processes and their properties will allow us to obtain a very detailed knowledge of the spin structure of the electroweak interaction for the top quark, knowledge which is not available from studies of the other heavy quarks, the c and b quarks. An important and instructive program of experimental work lies ahead of us, either by further use of the Tevatron, perhaps with increased luminosity, or by constructing a new hadronic collider at a significantly higher center-of-mass energy.

In hadronic collisions at high energy, the top and anti-top quarks are created as a pair, each with unknown momentum. The first question arising is how these top decay processes can be analyzed when the top quark's momentum is not known, especially as its most recognizable decay mode in the t -decay chain, $W \rightarrow l\nu_l$, involves the emission of a hard neutrino. In the above we have laid out a straightforward procedure of construction, which shows the nature and consequences of the information lacking and the degree of ambiguity in the analysis of the decay event. For an assumed laboratory energy E of the t quark, the missing neutrino momentum lies on a specific circular cone (traced out by the vector \mathbf{LX} in Fig. 5), each ray on the cone corresponding to a value for m_t (but with a twofold ambiguity, owing to the symmetry of the figure with respect to the plane of the vectors \mathbf{b} and \mathbf{l}). For an assumed m_t , with E unknown, the missing neutrino momentum lies on an elliptical cone (traced out by the vector \mathbf{LA} as A travels around the line of intersection between the paraboloid MON and the plane containing the line " $m_t = \text{const}$ " marked in Fig. 5); each point on this line " $m_t = \text{const}$ " corresponds to a different value of E (but with the twofold ambiguity just mentioned). The same construction may be made for the anti-top quark \bar{t} for $m_{\bar{t}}$. If the t and \bar{t} constructions are made for $m_{\bar{t}} = m_t$, using the same origin $\bar{P} = P$, the full $\bar{t}t$ event can thus be represented by two ellipses in space, one for t decay and the other for the \bar{t} decay. This implies that there is a double infinity of possible fits to the full event, even when the mass $m_{\bar{t}} = m_t$ is assumed known.

In $e^+e^- \rightarrow t\bar{t}$ there is an additional constraint, namely,

$$E_t = E_{\bar{t}} = E_e, \quad \mathbf{t} + \bar{\mathbf{t}} = 0. \quad (5.1)$$

How many solutions there can be when $m_{\bar{t}} = m_t$ is not known depends on the $(\mathbf{b}, \bar{\mathbf{l}})$ and $(\bar{\mathbf{b}}, \mathbf{l})$ configurations. The line of possible t solutions is now a circle (since $E = \bar{E} = \text{const}$), around which the value of m_t covers a definite range continuously; the line of possible \bar{t} solutions is another circle, not directly related with the t circle and generally corresponding to a different range of m_t . The question is whether or not there is a point X on the t cir-

cle and a point \bar{X} on the \bar{t} circle, both with the same value of m_t , such that the vectors \mathbf{PX} and $\mathbf{P}\bar{X}$ sum to zero, thus satisfying condition (5.1). In general, this will not be so, in which case the event is not due to $\bar{t}t$ creation. If the event does arise from $e^+e^- \rightarrow t\bar{t}$, there must be such an intersection; it will determine the top-quark mass and lead to the full identification of the event.

For hadronic $\bar{t}t$ creation, the resolution of the doubly infinite ambiguity requires more detailed assumptions. We appeal to the parton-antiparton description of the reaction. In the simplest parton model, the partons and antipartons move strictly parallel to the beam axis, so that the t and \bar{t} quarks created must then have total transverse momentum zero. However, in practice, it is found that the initial partons radiate some energy in the form of soft gluons and that this gives the final $\bar{t}t$ pair some small overall transverse momentum. We accepted only those fits with net transverse momentum less than one-tenth of the top-quark mass investigated. This still allows a double infinity of fits, but only over very limited ranges for the parameters which describe the final decay configuration. If no such fits were found, this would imply that the event is not due to $\bar{t}t$ creation. On the other hand, fits may exist even when the event is not $\bar{t}t$ production. This is the question of background, a matter which has not yet been discussed in the context of our event analysis, but which can be discussed by using this analysis with Monte Carlo-generated events for $b\bar{b}W^+W^-$ final states, such as Barger, Ohnemus, and Phillips [16] have generated in their discussions of other analysis procedures. Assuming that the events under discussion are really due to $\bar{t}t$ production, the probability for each configuration can be assessed as a function of m_t , as discussed in the above text, taking into account the proton structure function and lepton spectrum predicted for the sequence $t \rightarrow bW \rightarrow bl^+\nu_l$.

One good candidate event has existed for some time, from the work of the CDF group at the Fermilab Tevatron [12]. It is not known whether or not this event is necessarily an example of $\bar{t}t$ production, but we have used it as an illustration of our procedure. It may be of interest to note that, if this event is really a $\bar{t}t$ creation process with subsequent decays $t \rightarrow bW^+$ and $\bar{t} \rightarrow \bar{b}W^-$, then the top-quark mass lies in the range 115–144 GeV/ c^2 , its most probable value being 125 GeV/ c^2 .

ACKNOWLEDGMENTS

We wish to acknowledge valuable discussions with Dr. Krzysztof Sliwa about the CDF program of research. One of us (G.R.G.) acknowledges the U.S. Department of Energy for partial support during the course of this research and Dr. D. Sherrington for the hospitality of the Department of Theoretical Physics, University of Oxford; the other author (R.H.D.) wishes to acknowledge the continued hospitality of the Department of Theoretical Physics, under Professor D. Sherrington, and the hospitality of the Physics Department of Tufts University, Medford, MA, during two visits in the course of this work.

APPENDIX: A LOWER LIMIT FOR m_t

The covariant forms of (4.1) and (4.2) allow the derivation of an important inequality for m_t , given the four-momenta b and \bar{l} for the final b jet and lepton in the laboratory frame. These forms are

$$(t-b)^2 = (\bar{l} + \nu)^2 = M_W^2, \quad (\text{A1})$$

$$(t-b-\bar{l})^2 = (t-b)^2 - 2\bar{l} \cdot (t-b) + \bar{l}^2 = 0. \quad (\text{A2})$$

Taking $m_l = 0$ and inserting from the first expression, the latter equation takes the form

$$M_W^2 - 2\bar{l} \cdot \bar{t} + 2\bar{l} \cdot b = 0. \quad (\text{A3})$$

The scalar product $\bar{l} \cdot b$ in this equation can be evaluated from data in the laboratory rest-frame, whereas $\bar{l} \cdot t$ is given by $m_t E_{\bar{l}}$ in the t rest frame, where $E_{\bar{l}}$ is the lepton energy in that frame. The relations of momenta in these different frames are illustrated in Fig. 6.

An upper limit on $E_{\bar{l}}$ is readily obtained from a kinematic argument using only energy and momentum conservation, with the result

$$(E_{\bar{l}})_{\max} = (m_t^2 - m_b^2) / 2m_t. \quad (\text{A4})$$

After inserting these evaluations in (A3), we have

$$m_t = (\bar{l} \cdot b + M_W^2/2) / E_{\bar{l}} > (2\bar{l} \cdot b + M_W^2) 2m_t / (m_t^2 - m_b^2), \quad (\text{A5})$$

leading to the inequality

$$m_t > (m_b^2 + M_W^2 + 2\bar{l} \cdot b)^{1/2}. \quad (\text{A6})$$

A stronger inequality for $E_{\bar{l}}$ is obtained by considering the detailed chain $t \rightarrow bW$, $W \rightarrow \bar{l}\nu$, for which the upper limit on $E_{\bar{l}}$ is given by

$$E_{\bar{l}} \leq (Q_0 + |\mathbf{Q}|) / 2, \quad (\text{A7})$$

where Q_0 and \mathbf{Q} are given in the text above; Q_0 is equal to E_W , given in (3.12a), and $|\mathbf{Q}|$ is p , given by (3.12c). Using the inequality (A7) in Eq. (A5), some algebraic manipulations lead to the inequality

$$m_t > [(m_b^2 + 2\bar{l} \cdot b)(M_W^2 + 2\bar{l} \cdot b) / 2\bar{l} \cdot b]^{1/2}, \quad (\text{A8})$$

which is the optimal inequality, although it does not take into account the finite width Γ_W .

The inequality (A8) can place a significant limit on the minimum top-quark mass for a given (b, \bar{l}) pair, and this limit is used in the above text.

-
- [1] R. H. Dalitz, Gary R. Goldstein, and R. Marshall, *Phys. Lett. B* **215**, 783 (1988).
- [2] R. H. Dalitz, Gary R. Goldstein, and R. Marshall, *Z. Phys. C* **42**, 441 (1988).
- [3] CDF Collaboration, K. Sliwa, in *Z⁰ Physics*, Proceedings of the 25th Rencontre de Moriond, Les Arcs, France, 1990, edited by J. Tran Thanh Van (Editions Frontières, Gif-sur-Yvette, 1990), p. 459.
- [4] J. Ellis and G. H. Fogli, *Phys. Lett. B* **249**, 543 (1990).
- [5] I. I. Bigi, *Phys. Lett. B* **175**, 233 (1986).
- [6] I. Bigi, Y. Dokshitzer, V. Khose, J. Kühn, and P. Zerwas, *Phys. Lett. B* **181**, 157 (1986).
- [7] F. J. Gilman and R. Kauffman, *Phys. Rev. D* **37**, 2676 (1988).
- [8] See, for example, B. F. L. Ward, *Phys. Rev. D* **37**, 1865 (1988).
- [9] As this work was being written up, we received a paper by G. L. Kane, G. A. Ladinsky, and C.-P. Yuan, *Phys. Rev. D* **45**, 124 (1992). The thrust of our present paper is rather different from that of their paper, but there is naturally some overlap.
- [10] J. H. Kühn, *Nucl. Phys.* **B237**, 77 (1984).
- [11] A. Czarnecki, M. Jezabek, and J. H. Kühn, *Nucl. Phys.* **B351**, 70 (1991).
- [12] CDF Collaboration, F. Abe *et al.*, *Phys. Rev. Lett.* **64**, 147 (1990); CDF Collaboration, Lee Pondrom, in *Proceedings of the XXVth International Conference on High Energy Physics*, Singapore, 1990, edited by K. K. Phua and Y. Yamaguchi (World Scientific, Singapore, 1991), Vol. I, p. 144. We have used energy corrections and reference frame definitions provided by K. Sliwa (private communication).
- [13] CDF Collaboration, F. Abe *et al.*, *Phys. Rev. Lett.* **64**, 157 (1990).
- [14] UA2 Collaboration, P. Bagnaia *et al.*, *Phys. Lett.* **144B**, 283 (1984).
- [15] D. W. Duke and J. F. Owens, *Phys. Rev. D* **30**, 49 (1984).
- [16] V. Barger, J. Ohnemus, and R. J. N. Phillips, *Int. J. Mod. Phys. A* **4**, 617 (1989).